ChemComm

Accepted Manuscript

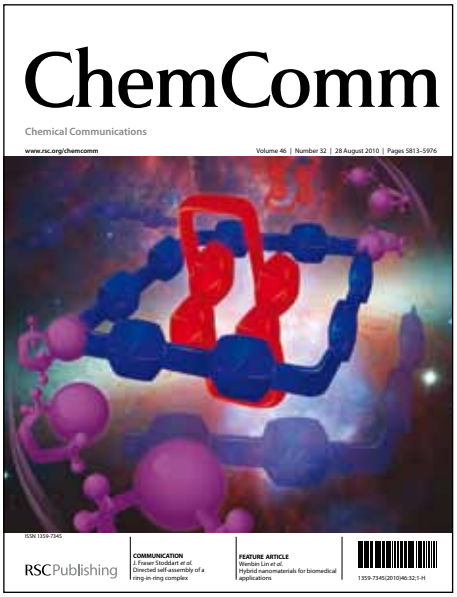

This is an *Accepted Manuscript*, which has been through the RSC Publishing peer review process and has been accepted for publication.

Accepted Manuscripts are published online shortly after acceptance, which is prior to technical editing, formatting and proof reading. This free service from RSC Publishing allows authors to make their results available to the community, in citable form, before publication of the edited article. This *Accepted Manuscript* will be replaced by the edited and formatted *Advance Article* as soon as this is available.

To cite this manuscript please use its permanent Digital Object Identifier (DOI®), which is identical for all formats of publication.

More information about *Accepted Manuscripts* can be found in the **Information for Authors**.

Please note that technical editing may introduce minor changes to the text and/or graphics contained in the manuscript submitted by the author(s) which may alter content, and that the standard **Terms & Conditions** and the **ethical guidelines** that apply to the journal are still applicable. In no event shall the RSC be held responsible for any errors or omissions in these *Accepted Manuscript* manuscripts or any consequences arising from the use of any information contained in them.

Cite this: DOI: 10.1039/c0xx00000x

www.rsc.org/xxxxxx

ARTICLE TYPE

In vivo ratiometric Zn^{2+} imaging in zerbrafish larva using a new visible light excitable fluorescent sensor

Zhipeng Liu,[a,b,‡] Changli Zhang,[a,c,‡] Yuncong Chen,[a] Fang Qian,[a] Yang Bai,[a] Weijiang He,[a,*] and Zijian Guo[a,*]

Received (in XXX, XXX) Xth XXXXXXXXX 20XX, Accepted Xth XXXXXXXXX 20XX

DOI: 10.1039/b000000x

A visible light excitable ratiometric Zn^{2+} sensor was developed by integrating a Zn^{2+} chelator as ICT donor of fluorophore sulfamoylbenzoxadiazole, which displays the Zn^{2+}-induced hypsochromic emission shift (40 nm) and favors the in vivo ratiometric Zn^{2+} imaging in zerbrafish larva.

Labile Zn^{2+} is attracting much more interests since it is associated with both the physiological progresses such as neurotransmission and gene transcription, [1] and the pathophysiology of certain diseases.[2] Fluorescent Zn^{2+} imaging with Zn^{2+} sensors has demonstrated great success in providing temporal-spatial information of Zn^{2+} homeostasis in live cells .[3] Since the cellular Zn^{2+} biology is far from the complicated Zn^{2+} physiology in advanced organisms, the in vivo Zn^{2+} imaging in living animal models is especially demanded. As a valuable vertebrate model of high homology with mammals, zebrafish embryo or larva benefits the studies of development biology, molecular genetics, neuroscience, signal transduction, and pathology from the small size and optically transparency for in vivo imaging.[4] Moreover, the controlled external fertilization enables the in vivo imaging during all stages of embryonic development. Therefore, developing Zn^{2+} sensor especially those of long excitation wavelength to promote the in vivo Zn^{2+} imaging in zebrafish larvae is one of the most interested areas in this field, and several turn-on sensors have been applied for Zn^{2+} imaging in live zebrafish larva after our first report.[5] However, this turn-on in vivo Zn^{2+} imaging suffers still from the interferences induced by the altered sensor concentration, autofluorescence, bleaching, etc. More accurate Zn^{2+} imaging in zebrafish larva is ratiometric Zn^{2+} imaging demanding the ratiometric Zn^{2+} sensors of visible light/NIR excitability.

In this communication, we report a visible light excitable ratiometric Zn^{2+} sensor **SBD-TPEA**, which has been utilized for the first in vivo ratiomertic Zn^{2+} imaging in zebrafish larva. This sensor was constructed with a mechanism of metal coordination altering ICT (intramolecular charge transfer) effect in fluorophore, which is an effective design rationale for ratiometric metal ion sensors.[6] In this sensor, the Zn^{2+} chelator, TPEA (*N,N,N'*-tri(pyridin-2-ylmethyl)ethane-1,2-diamine), was incorporated into an ICT fluorophore **ASBD** (4-amine-7-sulfamoylbenzo[c][1,2,5]oxadiazole) acting as both the ICT donor group and Zn^{2+} ionophore. This sensor was prepared in a moderate yield by reacting SBD-Cl with TPEA via a SN_{Ar} substitution (Scheme 1, please see also Supplementary Information).

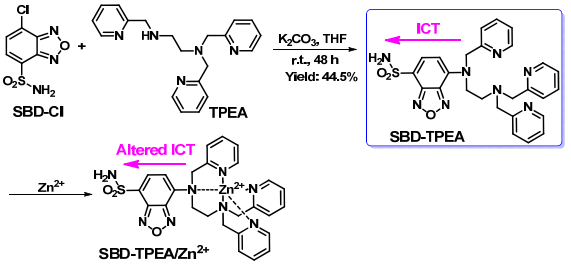

Scheme 1. Synthesis of **SBD-TPEA** and its Zn^{2+} complexation.

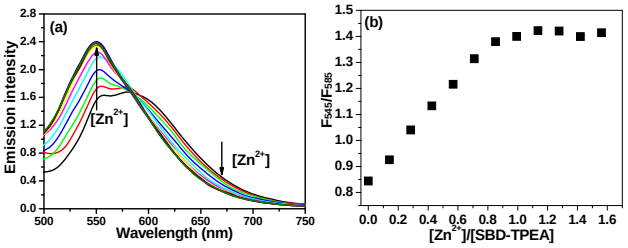

Fig. 1. (a) Emission spectra of 3 μM **SBD-TPEA** (λ_{ex}, 460 nm) in HEPES buffer (50 mM, 0.1 M KNO_3, pH 7.2, containing 0.15% DMSO) obtained by adding aliquots of Zn^{2+} solution (1.2 mM, 1.1 μL); (b) the titration profile according to the ratio of emission at 545 nm to that at 585 nm, F_{545}/F_{585}.

The sensor is able to be dissolved in water with a concentration up to ~ 3.0 μM according to a reported determination procedure (Fig. S7).[7] The spectroscopic determination of **SBD-TPEA** were carried out in HEPES buffer (50 mM HEPES, 100 mM KNO_3, pH 7.2) containing 0.15 % DMSO. **SBD-TPEA** exhibits an emission band centered at 585 nm, with an excitation maximum at 466 nm. The large Stokes shift (119 nm) is helpful to reduce the excitation interference in imaging. Fluorescence Zn^{2+} titration of **SBD-TPEA** displayed a distinct hypsochromic emission shift from 585 to 545 nm with an isoemission point at 585 nm (Fig. 1a). The ratio of emission at 545 nm to that at 585 nm (F_{545}/F_{585}) increases linearly from 0.85 to 1.42 with $[Zn^{2+}]_{total}$ till the $[Zn^{2+}]_{total}$/[**SBD-TPEA**] ratio attains to 1 : 1 (Fig. 1b). Even higher $[Zn^{2+}]_{total}$ does not lead to any evident change in emission. The excitation and emission maxima for both apo- and Zn^{2+}-bound sensors are located in the range of

visible light, favouring the in vivo imaging in zebrafish larva. Fluorescence pH titration demonstrated that F_{454}/F_{585} of **SBD-TPEA** has no pH-dependence in the pH range from 6.5 to 9.0, favoring its ratiometric imaging application in physiological microenvironments (Fig. S8). In addition, the Zn^{2+}-induced emission enhancement for **SBD-TPEA** is limited, suggesting there is no distinct PET (photo-induced electron transfer) effect from Zn^{2+} ionophore to the parent fluorophore, **ASBD**.[6a]

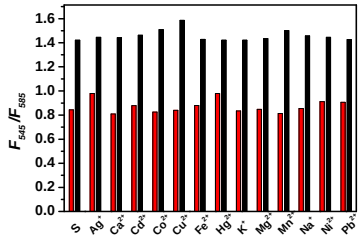

Fig. 2. Ratio of emission at 545 to that at 585 nm, F_{545}/F_{585}, of **SBD-TPEA** (3 μM) in HEPES buffer (0.15% DMSO, 50 mM HEPES, 100 mM KNO_3; pH 7.20) induced by different metal cations. Red bars, ratio for free sensor (S) or in the presence of 1 equiv Ag^+, Cd^{2+}, Co^{2+}, Cu^{2+}, Fe^{2+}, Hg^{2+}, Mn^{2+}, Ni^{2+}, Pb^{2+} or 1000 equiv Na^+, K^+, Ca^{2+}, Mg^{2+}. Black bars, ratio in the presence of Zn^{2+} (1 equiv), or the indicated metal ions (1 equiv) followed by adding 1 equiv Zn^{2+}. λ_{ex}, 460 nm.

The UV-vis Zn^{2+} titration of **SBD-TPEA** demonstrated an absorption shift from 456 (Band A, ε, 4.46×10^3 $M^{-1}cm^{-1}$) to 386 nm (Band B, ε, 3.29×10^3 $M^{-1}cm^{-1}$, Fig. S9). The linear decrease of Band **A** and increase of Band **B** with $[Zn^{2+}]_{total}$ can be observed simultaneously till the $[Zn^{2+}]_{total}$/[**SBD-TPEA**] ratio attains to 1 : 1. Even higher zinc concentration does not lead to any further change. The UV-vis titration profiles according to the absorbance of the two bands and the clear isobestic point at 416 nm suggest that Zn^{2+} addition led to only one reaction to form sole Zn^{2+} complex of 1:1 stoichiometry. ^1H NMR titration by Zn^{2+} confirmed also the 1:1 Zn^{2+} binding stoichiometry of **SBD-TPEA** (Fig. S10), and all N atoms in TPEA are involved in Zn^{2+} coordination directly (Figs. S10-S12, Table S1 and Chart S1). MS determination of **SBD-TPEA**/Zn^{2+} complex confirmed again the 1:1 Zn^{2+} binding stoichiometry (Fig. S6). The data obtained from the two Zn^{2+} titrations implied that Zn^{2+} coordination to TPEA amine N attached to benzoxadiazole decreases the ICT effect of **ASBD** fluorophore and induces the hypsochromic shift of absorption and emission.

The Zn^{2+}-specific ratiometric response of **SBD-TPEA** was confirmed further by fluorescence titration with biorelated metal cations of interest. As shown in Fig. 2, the presence of Na^+, K^+, Ca^{2+}, and Mg^{2+}, which are abundant in cells, does not interfere with its ratiometric response to Zn^{2+}, even though their concentration is 1000 times higher than $[Zn^{2+}]_{total}$. In addition, the presence of Ag^+, Fe^{2+}, Hg^{2+}, Ni^{2+}, Mn^{2+} Co^{2+}, Cd^{2+}, Cu^{2+}, and Pb^{2+} (1 equiv) does not interfere with its ratiometric sensing ability to Zn^{2+}. The K_d value of Zn^{2+}/**SBD-TPEA** complex was estimated to be ~ 2.1 nM *via* determining the Zn^{2+}-induced change of F_{545}/F_{585} ratio in a series of Zn^{2+} buffer solutions (Fig. S13). [8] The detection limit (3σ/slope) of this sensor was determined to be 0.5 nM (Fig. S14). All these make **SBD-TPEA** a suitable candidate of ratiometric imaging agent for intracellular and in vivo Zn^{2+}.

The intracellular Zn^{2+} imaging ability of **SBD-TPEA** was investigated in HepG2 cells using confocal microscope with a dual emission mode (green channel: 510–560 nm; red channel: 580–630 nm) upon excitation at 488 nm, and the ratiometric images were obtained by mediating the green channel image with the related red channel image (Fig. S15). As shown in Fig. 3, the cells stained by **SBD-TPEA** display the faint green/blue (lower ratio) in cytoplasm in the ratiometric image, indicating the labile Zn^{2+} level in cytoplasm is low. When exogenous Zn^{2+} was introduced *via* incubation the cells with $ZnSO_4$/pyrithione solution (5 μM, 1:2), the intensive blue was observed inside the cell, indicating the enhanced intracellular Zn^{2+} level. According the ratio bar, the red/yellow spots close to the nucleus indicate that the Zn^{2+} level in these regions is even higher. The followed incubation treatment with the cell membrane permeable Zn^{2+} chelator, *N*,*N*,*N'*,*N'*-tetrakis(2-pyridylmethyl)ethylenediamine (TPEN), displayed very minor green area inside the cells, implying the distinctly suppressed emission ratio and lower Zn^{2+} level than that in original cells in Fig. 3b. These results also confirmed that the fluorescence ratio enhancement in cells upon $ZnSO_4$/pyrithione incubation should be resulted from Zn^{2+} binding of **SBD-TPEA**, and the intracellular Zn^{2+} level can be enhanced effectively via Zn^{2+} incubation. Similar results were obtained also in HeLa cells (Fig. S16), and the higher Zn^{2+} level was also observed in the regions close to nucleus when exogenous Zn^{2+} was introduced. Co-localization experiments in HeLa cells (Fig. S17) and HepG2 cells *via* co-staining the cells with **SBD-TPEA** and Golgi maker BODIPY TR ceramide disclosed that the bright spots of higher Zn^{2+} level are Golgi apparatus. In addition, the chelatable $[Zn^{2+}]$ in Golgi of HepG 2 cells was estimated to be around 0.5 nM (Fig. 3 and Fig. S15). The ratiometric imaging results suggest also that the average chelatable Zn^{2+} level in HepG2 cells is different from that in HeLa cells. Moreover, the temporal imaging of cells treated by **SBD-TPEA** displayed no change in cell morphology in 4 h, implying the fine biocompatibility of **SBD-TPEA**.

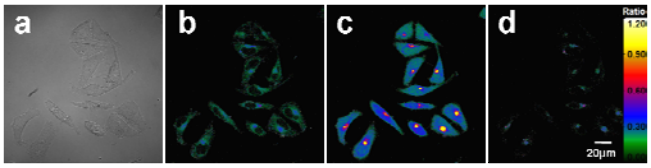

Fig. 3. Confocal fluorescence ratiometric imaging of HepG2 cells stained by **SBD-TPEA** (10 μM, 20 min) at 25 °C. (a) Bright-field transmission image of the stained cells; (b) ratiometric image of cells in (a); (c) ratiometric image of cells in (b) exposed to $ZnSO_4$/pyrithione solution (5 μM, 1:2) for 5 min, followed by staining again with **SBD-TPEA** solution; (d) ratiometric image of cells in (c) treated by TPEN solution (25 μM, 10 min). Ratiometric images were obtained via mediating the fluorescence images collected respectively at green channel (510–560 nm) and red channel (580–630 nm). λ_{ex}, 488 nm.

Besides the ratiometric Zn^{2+} imaging ability in living cells of **SBD-TPEA**, the first ratiometric in vivo Zn^{2+} imaging in 3-day-old zebrafish larva was also investigated via staining the larva by **SBD-TPEA** (50 μM, 1.5 h) . As shown in Fig. 4a, the confocal fluorescence images of the larva head exhibit mainly two regions of bright fluorescence, and the overlay of fluorescence and bright-field images discloses the two bright regions are symmetrically located between the two eyes, which was proposed as the neuromasts of the anterior lateral-line system (ALL system) in zebrafish. [9] The ratiometric image obtained via mediating

fluorescence images obtained respectively from band paths 550-560 and 570-650 nm displays the pale blue regions on the same location, indicating the higher Zn^{2+} level in these two bright spots than that in the rest of the head (Fig. 4a-4d). The ratiometric imaging of Zn^{2+}-fed zebrafish larva (3-day-old) has also been carried out by incubating larva with Zn^{2+} solution for 1 h (100 μM), and the ratiomertic image demonstrates two bright cyan spots in the same location (Fig. 4e-4h). Moreover, the two cyan regions are larger than the pale blue regions found in the non-Zn^{2+}-fed larva, and the bright cyan implies that the neuromast Zn^{2+} level in Zn^{2+}-fed larva is higher than that in non-Zn^{2+}-fed larva. The TEPN (50 μM, 0.3 h) treatment of the **SBD-TPEA** stained 3-day-old zebrafish larva (50 μM, 1.5h) results in almost dim images and the fluorescence in the nuromast is very low. In addition, only very minor faint pale blue spots can be found in the corresponding areas in ratiometric image (Fig. 4i-4l). Comparison between the ratiometric images of the normal zebrafish larva and the TPEN treated larva suggests that the two pale blue regions in the normal zebrafish larva should be correlated to the presence of higher labile Zn^{2+} level. All the altered emission ratio displayed as the variable color in the ratiometric image is really correlated to the variable chelatable Zn^{2+} level in live zebrafish larva. The ratiometric imaging results on 5 zebrafish larvae disclosed that the chelatable [Zn^{2+}] of neuromasts is around 1.3 nM, while the Zn^{2+}-incubation made the [Zn^{2+}] in the corresponding regions increase to 10.9 nM. As to the TEPN treated larva, the chelatable [Zn^{2+}] in neuromast can be reduced to 0.1 nM (Fig. S18). All the preliminary imaging data indicate that **SBD-TPEA** is an effective Zn^{2+} ratiometric sensor for *in vivo* Zn^{2+} quantitative imaging.

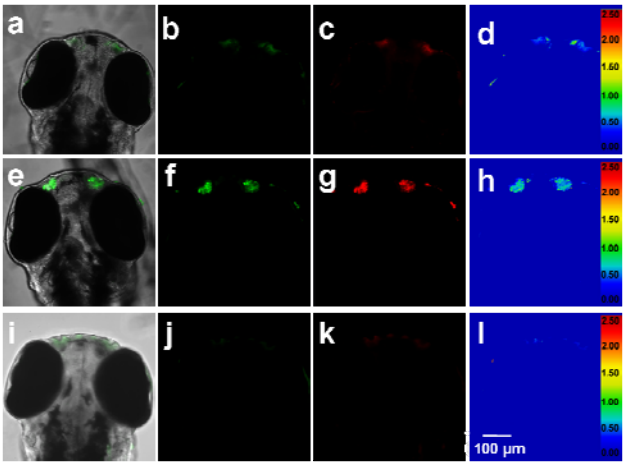

Fig. 4. Confocal fluorescence ratiometric Zn^{2+} imaging in the head of three-day-old zebrafish larva at 28.5ºC. (a-d) Images of a larva incubated with **SBD-TPEA** (50 μM,1.5 h); (e-h) images of a larva fed with Zn^{2+} (100 μM, 1h) solution followed by incubation with **SBD-TPEA** (50 μM, 1.5 h); (i-l) images of a larva incubated with **SBD-TPEA** (50 μM, 1.5 h) followed by 20 min of TPEN incubation (50 μM). (a, e, i) Colocalization of bright-field and fluorescence images for the head (dorsal view); (b, f, j) fluorescence images from band path 500–560 nm; (c, g, k) fluorescence images from the band path 570–650 nm; (d, h, i) ratiometric images generated from (b, f, j) and (c, g, k). λ_{ex}, 488 nm.

In conclusion, a novel ratiometric Zn^{2+} fluorescent sensor **SBD-TPEA** derived from ICT fluorophore **ASBD** was developed. This new sensor displays the specific Zn^{2+}-induced emission shift from 585 to 545 nm, which provides the sensor the ratiometric Zn^{2+} sensing ability. With the pH-independent sensing behavior in physiological pH range and visible light excitability, **SBD-TPEA** has been utilized to realize the in vivo ratiometric Zn^{2+} imaging in live zebrafish larva for the first time, and the chelatable Zn^{2+} level of the nuromasts in the larva head was firstly estimated.

We thank the National Basic Research Program of China (No. 2011CB935800), National Natural Science Foundation of China (No. 21271100, 21131003, 21021062, and 91213305) and Natural Science Foundation of Shandong Province (ZR2011BQ010) for financial support.

Notes and references

[a] *State Key Laboratory of Coordination Chemistry, Coordination Chemistry Institute, School of Chemistry and Chemical Engineering, Nanjing University, Nanjing 210093, P. R. China. Email:heweij69@nju.edu.cn; zguo@nju.edu.cn; Fax: +86 25 83314502; Tel: +86 25 83597066.*

[b] *Department of chemistry, Liaocheng Unviersity, Liaocheng, 252059, P. R. China.*

[c] *Department of chemistry, Nanjing Xiaozhuang College, Nanjing, 210017, P. R. China.*

[d] *Animal Model Research Center, Nanjing University, Nanjing 210061, P. R. China.*

† Electronic Supplementary Information (ESI) available: Synthesis of **SBD-TPEA**, spectroscopic studies and experimental details. See DOI: 10.1039/b000000x/.

‡ *Both authors contributed equally to this manuscript.*

[1] (a) J. M. Berg and Y. Shi, *Science*, 1996, **271**, 1081; (b) M. Lu and D. Fu, *Science*, 2007, **317**, 1746.

[2] (a) C. J. Frederickson, J.-Y. Koh and A. I. Bush, *Nat. Rev. Neurosci.*, 2005, **6**, 449; (b) M. Cortesi, R. Chechik, A. Breskin, D. Vartsky, J. Ramon, G. Raviv, A. Volkov and E. Fridman, *Phys. Med. Biol.,* 2009, **54**, 781.

[3] (a) E. Tomat and S. J. Lippard, *Curr. Opin. Chem. Biol.*, 2010, **14**, 225; (b) Z. Xu, J. Yoon and D. R. Spring, *Chem. Soc. Rev.*, 2010, **39**, 1996; (c) E. L. Que, D. W. Domaille and C. J. Chang, *Chem. Rev.*, 2008, **108**, 1517; (d) P. Jiang and Z. Guo, *Coord. Chem. Rev.*, 2004, **248**, 205.

[4] (a) S. Ellingsen, M. A. Laplante, M. Konig, H. Kikuta, T. Furmanek, E. A. Hoivik and T. S. Becker, *Development*, 2005, **132**, 3799; (b) H. W. Detrich, M. Westerfield and L. I. Zon, *The zebrafish: disease models and chemical screens*, academic Press, Waltham, 3rd edn, 2011; (c) L. A. Trinh and S. E. Fraser, *Dev. Growth Differ.*, 2013, **55**, 434; (d) S. Rinkwitz, P. Mourrain and T. S. Becker, *Prog. Neurobiol.*, 2011, **93**, 231; (e) S.-K. Ko, X. Chen, J. Yoon and I. Shin, *Chem. Soc. Rev.*, 2011, **40**, 2120.

[5] (a) F. Qian, C. Zhang, Y. Zhang, W. He, X. Gao, P. Hu and Z. Guo, *J. Am. Chem. Soc.*, 2009, **131**, 1460; (b) Z. Xu, K.-H. Baek, H. N. Kim, J. Cui, X. Qian, D. R. Spring, I. Shin and J. Yoon, *J. Am. Chem. Soc.*, 2010, **132**, 601; (c) J. E. Kwon, S. Lee, Y. You, K.-H. Baek, K. Ohkubo, J. Cho, S. Fukuzumi, I. Shin, S. Y. Park and W. Nam, *Inorg. Chem.*, 2012, **51**, 8760; (d) K. Jobe, C. H. Brennan, M. Motevalli, S. M. Goldup, M. Watkinson, *Chem. Commun.*, 2011, **47**, 6036; (e) Y. Xu, Q. Liu, B. Dou, B. Wright, J. Wang and Y. Pang, *Adv. Healthcare Mater.*, 2012, **1**, 485.

[6] (a) Z. Liu, W. He and Z Guo, *Chem. Soc. Rev.,* 2013, **42**, 1568; (b) L. Xue, G. Li, D. Zhu, Q. Liu and H. Jiang, *Inorg. Chem.*, 2012, **51**, 10842; (c) L. Xue, G. Li, D. Zhu, C. Yu and H. Jiang, *Chem. Eur. J.*, 2012, **18**, 1050; (d) Z. Liu, C. Zhang, Y. Chen, W. He and Z. Guo, *Chem. Commun.*, 2012, **48**, 8365.

[7] H. M. Kim, M. S. Seo, M. J. An, J. H. Hong, Y. S. Tian, J. H. Choi, O. Kwon, K. J. Lee and B. R. Cho, *Angew. Chem. Int. Ed.,* 2008, **47**, 5167.

[8] M. Taki, J. L. Wolford and T. V. O'Halloran, *J. Am. Chem. Soc.*, 2004, **126**, 712.

[9] K. A. Grant, D. W. Raible and T. Piotrowski, *Neuron,* 2005, **45**, 69.